

Theory and Performance of Narrow Correlator Spacing in a GPS Receiver

A. J. VAN DIERENDONCK

AJ Systems, Los Altos, California

PAT FENTON and TOM FORD

NovAtel Communications Ltd., Calgary, Alberta

Received January 1992

Revised June 1992

ABSTRACT

Historically, conventional GPS receivers have used 1.0 chip early-late correlator spacing in the implementation of delay lock loops (DLLs). However, there are distinct advantages to narrowing this spacing, especially in C/A-code tracking applications. These advantages are the reduction of tracking errors in the presence of both noise and multipath. The primary disadvantage is that a wider precorrelation bandwidth is required, coupled with higher sample rates and higher digital signal processing rates. However, with current CMOS technology, this is easily achievable and well worth the price.

Noise reduction is achieved with narrower spacing because the noise components of the early and late signals are correlated and tend to cancel, provided that early and late processing are simultaneous (not dithered). Multipath effects are reduced because the DLL discriminator is less distorted by the delayed multipath signal.

This paper presents the derivation of these narrow correlator spacing improvements, verified by simulated and tested performance.

INTRODUCTION AND BACKGROUND

The use of 1.0 (or even 2.01 chip correlator spacing in delay lock loops (DLLs) dates back to the early GPS receivers, starting with the Phase I GPS X-Set, Y-Set, Z-Set, and Manpack. In early theoretical papers, 1.0 chip spacing was implied [1,2]. Narrower spacing was mentioned in the classic multipath effects report [2], but not in a complimentary way. However, this dishonorable mention was with respect to coherent DLLs in the presence of strong multipath. For multipath signals of more reasonable levels, these adverse effects are not true, nor are they true for noncoherent DLLs. This has been verified [3], and is explained herein.

The 1.0 chip spacing concept carried over to the GPS Phase II and Phase III equipment, and more recently to modern digital GPS receivers [4,5]. Although these cited receivers are of the P-code variety, this 1.0 chip spacing concept has also been used in most commercial C/A-code receivers. In fact, it has been such a standard approach that authors of papers describing their designs do not even mention the spacing, except that it is implied by their performance equations and test results.

In the early days of GPS, there were a number of reasons why the 1.0 chip spacing was used. Some of these reasons are as follows:

- 1) This was a normal analog implementation in the early days to minimize hardware. The advantages in noise are not present if a T-dither DLL is used. This is because the early and late noise components are uncorrelated as a result of time-independence. A r-dither DLL is one that time-shares a correlator between the early and late signals. However, most receivers today, if not all, perform early and late (or early-minus-late) correlation simultaneously .
- 2) The early receivers were usually of the P-code variety, Since the P-code chip is already relatively short, narrower spacing makes the DLL discriminator quite narrow. It was feared that Doppler and other disturbances would cause loss of code lock. Carrier aiding of the DLL minimizes this problem. Carrier aiding was implemented in the early receivers, but the designers of those receivers feared the effects of jamming at initial DLL acquisition. However, the linear range of a C/A-code DLL discriminator is 10 times greater than that of a P-code discriminator. Thus, this reason does not have a foundation in carrier-aided C/A-code applications, except possibly during DLL acquisition. However, variable spacing eliminates that problem.
- 3) Narrower spacing requires faster clocking of the early/late gating. This presented a technology problem, especially using the P-code. In fact, it is still somewhat of a problem in P-code applications. However, in the case of a C/A-code receiver, the chipping rate is 1/10 that of a P-code receiver. Today's technology easily accommodates the clocking for narrower spacing in a C/A-code receiver.
- 4) It is speculated that most designers failed to realize the potential of narrower spacing. The results presented in this paper eliminate this problem.

The reasons for 1.0 chip correlator spacing in a C/A-code DLL have all been eliminated, and variable spacings have been implemented in the new NovAtel GPSCardtm [6]. This receiver has a variable correlator spacing capability, with the ability to vary the spacing of the early and late reference code from 0.05 to 1.0 C/A-code chip. The C/A-code tracking noise performance of that receiver is better than 10 cm, one sigma, using DLL loop bandwidths of 0.1 Hz or less at nominal signal-to-noise ratios.

This superior C/A-code tracking performance is the primary reason for the implementation of the narrow spacing. A derivation of that performance and test results are presented below, showing tracking performance essentially equivalent to P-code tracking. However, when this concept was first presented [6], questions were raised about the tracking performance in the presence of multipath, which is usually the limitation of accuracy in surveying and kinematic surveying applications using the C/A-code. This prompted our analysis and testing of the effects of multipath. The results of that analysis and testing are also presented in this paper. Those results show superior performance in the presence of multipath, approaching that obtainable using a P-code receiver.

DLL NOISE PERFORMANCE

The derivation of the DLL noise performance as a function of correlator spacing is presented in the appendix. That derivation is based on a GPS receiver correlator implementation shown in Figure 1, which describes the generation of early, punctual, and late codes. Note that the notations used in the following equations are defined in the appendix.

Generation of Early, Punctual, and Late Codes

In a modern digital GPS receiver, DLL discriminators are based on in-phase (I_k) and quadrature (Q_k) samples of a filtered signal $S_f(t)$ at baseband, cross-correlated with the reference PN code. The form of these samples is presented in the appendix. The cross-correlation process is illustrated in Figure 1. In the implementation presented, both the incoming I and Q samples are correlated either with the early (E) and late (L) reference codes (called the early-minus-late power mode), or with the punctual (P) and early-minus-late (E-L) reference codes (called the dot-product mode). These modes of operation are selectable with a discriminator select command. This selection allows the implementation of at least three types of DLL discriminators—two noncoherent and one coherent.

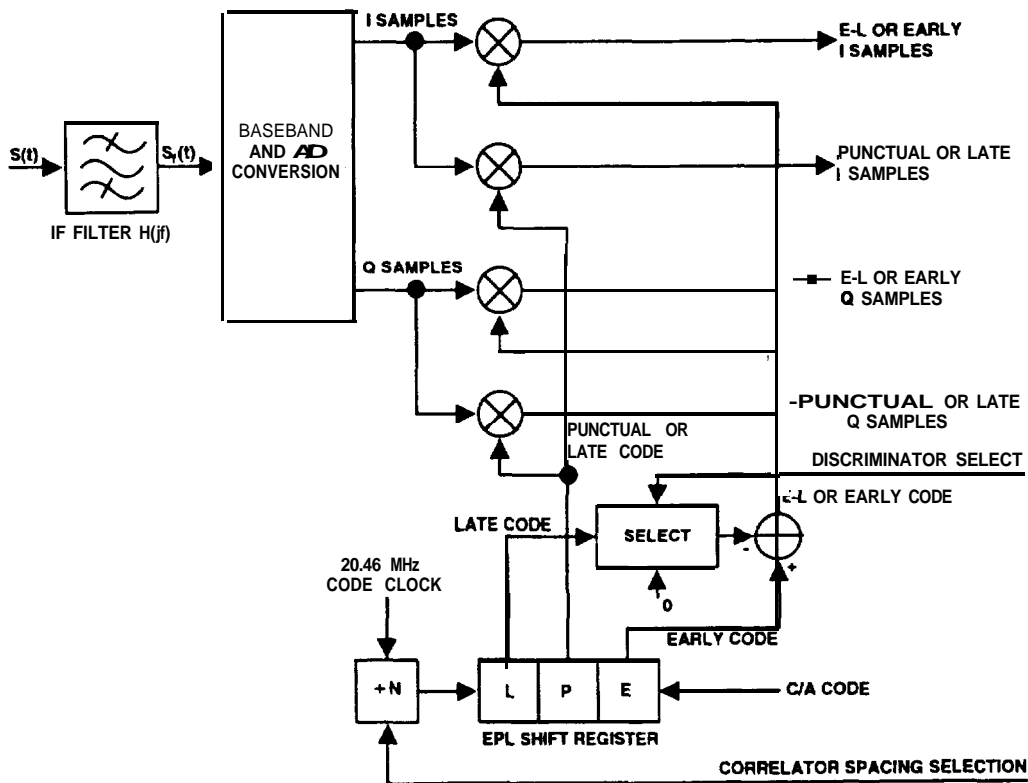


Fig. 1 - GPS Digital Receiver Cross-Correlation Process

DLL Discriminators

The two noncoherent discriminators of interest are as follows:

$$d\tau_k = I_{E_k}^2 + Q_{E_k}^2 - I_{L_k}^2 - Q_{L_k}^2 \quad (1)$$

in the early-minus-late power mode, and

$$d\tau_k = I_{E-L,k} I_{Pk} + Q_{E-L,k} Q_{Pk} \quad (2)$$

in the dot-product mode. A typical coherent discriminator takes on the form

$$d\tau_k = I_{E-L,k} \text{sign}(I_{Pk}) \quad (3)$$

where $\text{sign}(I_{Pk})$ represents the sign of the GPS navigation message data bit at time t_k , and $d\tau_k$ is the discriminator value. Note that the coherent discriminator requires that the receiver be phase-locked to the signal. Although this coherent implementation may save hardware (no quadrature channel is required for the E-L or early samples), signal acquisition and reacquisition performance is degraded without that hardware. As shown in the appendix, there is little if no performance advantage in using the coherent discriminator. In fact, there is a significant performance disadvantage if carrier phase cycle slipping occurs.

Correlator Spacing

The key concept illustrated in Figure 1 is the selection of the shift register clock that generates the early, punctual, and late codes. N can take on values from 1 to 20 to provide a variable spacing between those codes, resulting in early-late code spacing from 0.05 to 1.0 C/A-code chip, depending upon operating mode. This mechanization allows for a minimum E/L correlator spacing of 0.05 C/A-chip in the early-minus-late power mode and 0.1 C/A-chip in the dot-product or coherent modes.

SIMULATION AND TEST RESULTS

Band Limiting Effects

The performance of a DLL with narrow correlator spacing is very much influenced by the precorrelation bandwidth. This is because band limiting tends to round the autocorrelation peak; thus the discrimination between early and late correlation is limited when using very narrow correlator spacing. To verify this connection, a simulation was developed using filtered cross-correlation functions such as presented in equation (A-3) of the appendix. More extensive models than those presented in equations (A-1) and (A-2) of the appendix were used to include carrier loop simulations as well, by adding frequency error dependence to the model. The precorrelation filter was modeled as a 5th-order Butterworth filter. The actual filter in the GPSCardTM is a surface acoustic wave (SAW) filter, for which test results are presented below. In either case, the filters both exhibit substantial roll-off outside of the bandwidth. Thus, their effects on the filtered signal spectral density are very similar.

Discriminator Simulation

Before closing the DLL tracking loop, simulations were run to map discriminator versus correlator spacing d and code offset τ_k . Figure 2 presents a typical mapping for the early-minus-late power discriminator with 0.05 chip correlator spacing, normalized with the sum of early and late power, which is the implementation we use instead of automatic gain control. This is why the discriminator peaks at large code offsets, making it difficult to break lock at higher signal-to-noise ratios. These peaks diminish because of noise suppression at lower signal-to-noise ratios. Figure 3 shows a closer view of that simulated early-

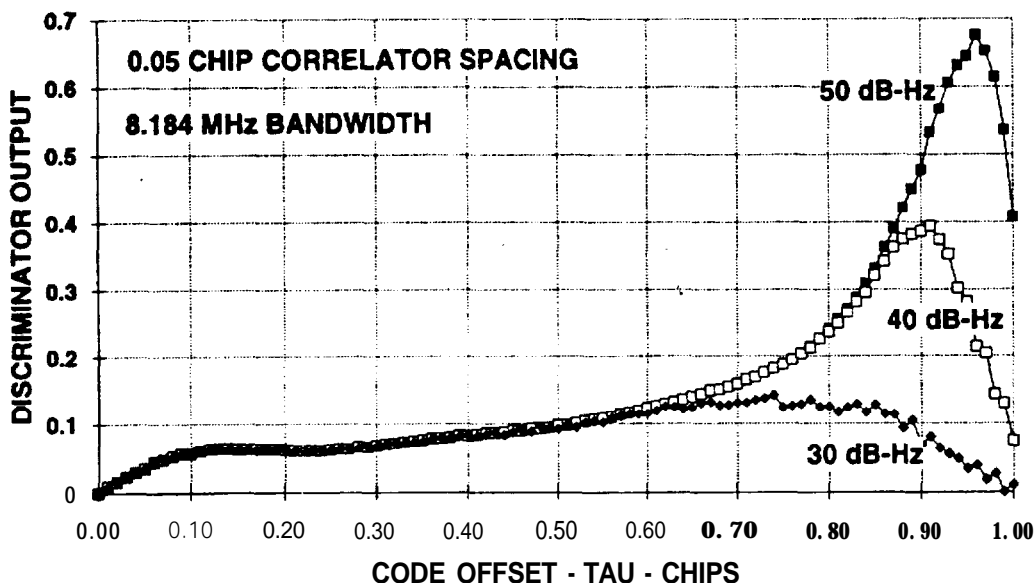


Fig. 2-Simulated Early-Minus-Late Power Discriminator for 0.05 Chip Spacing

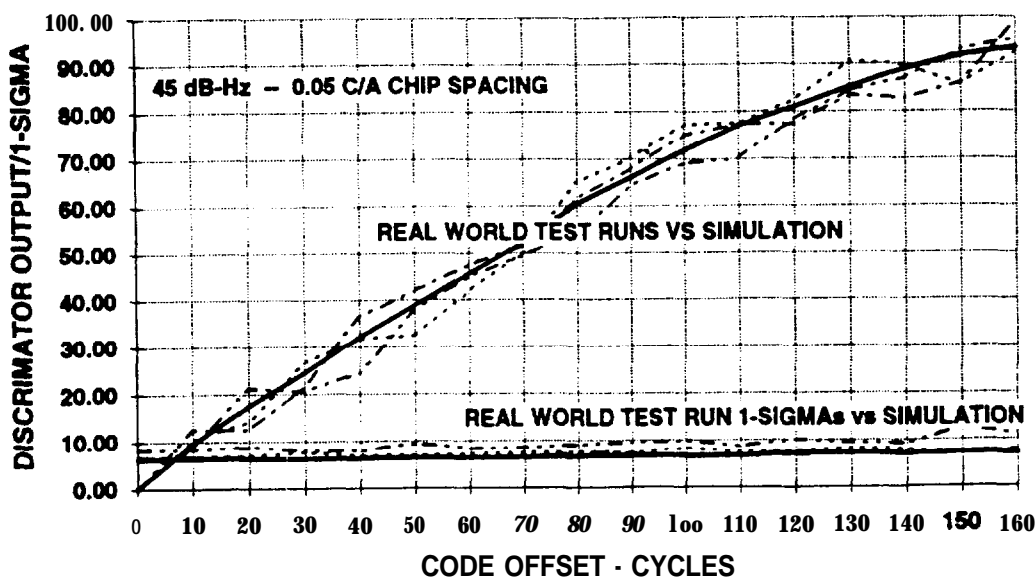


Fig. 5-Early-Minus-Late Power Discriminator Simulated Versus Test Results (noise only)

minus-late power discriminator at a C/N_0 of 45 dB-Hz versus real-world test data. This figure illustrates the integrity of the simulation and shows that we do indeed have discrimination with the narrow 0.05 chip spacing. However, the results that follow show there is a diminishing return using very narrow correlator spacing for the bandwidths employed. Thus, even though the use of the early-minus-late power discriminator allows one to have a narrower spacing, we choose not to use it operationally. Then, using the dot-product mode, we have a punctual correlator available for carrier tracking. The results hereafter are given for that mode of operation.

Test Results

Real-world test data **were** collected by locking on to a satellite signal, achieving steady-state tracking, and then opening the DLL by using carrier aiding only. Each of the 10 channels was assigned a different correlator spacing d , ranging from 0.1 to 1.0 chip. In this way, we accomplished two things. First, we collected discriminator data for the different correlator spacings. Second, we offset the code in steps and mapped the discriminator function to determine its characteristics. The time limit of this process was constrained by the time for code-carrier divergence due to the ionosphere.

Figure 4 presents the gain of the dot-product discriminator normalized with the punctual power

$$P_k = I_{Pk}^2 + Q_{Pk}^2 \quad (4)$$

where, for infinite bandwidth using the I and Q models of the appendix,

$$E[P_k] = 2 S/N_0 T (1 - |\tau_k|)^2 + 2 \quad (5)$$

where $E[-]$ is the expected value operator.

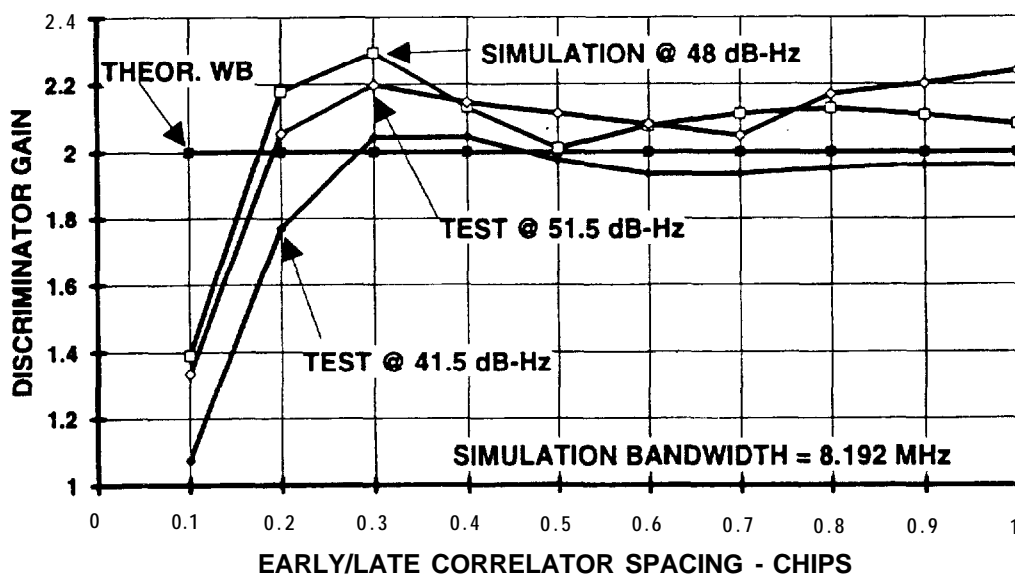


Fig. 4-Bandwidth Effects on Dot-Product Discriminator Gain Versus Correlator Spacing

At high signal-to-noise ratio, the normalized infinite bandwidth discriminator gain is 2, which represents a normalized version of the quantity (discriminator gain)

$$G_d = \frac{E[d\tau_k]}{\tau_k} \Big|_{k=0} \tag{6}$$

Using the relationship of equation (A-27) of the appendix in conjunction with equation (A-31) of the appendix, the one-sigma tracking loop noise performance can also be estimated as

$$a_s = \frac{\sqrt{2B_L T}}{G_d} \sigma_{dr} \tag{7}$$

This method of estimating tracking performance is very useful since each discriminator output is statistically independent in time. In that way, statistics can be computed on many independent samples in a short period of time, as opposed to using statistically independent closed-loop samples from narrow-band tracking loops.

The simulated and tested gains presented in Figure 4 are certainly close to the theoretical gain, except at the very narrow spacings, because of band limiting. However, the test data gains agree quite well with the simulated data gains. Some noise suppression is evident at 41.5 dB-Hz.

The performance parameter of equation (7) is plotted in Figure 5, along with the wideband theoretical case for the simulation and test results for a loop bandwidth of 1 Hz. Again, the simulation and test results agree very well, but deviate at the narrow spacings due to band limiting. In fact, the results show that a spacing of 0.2 chip performs as well as or better than a spacing of 0.1 chip for the 8 MHz bandwidth. Both spacings are much better than a 1.0 chip spacing, however.

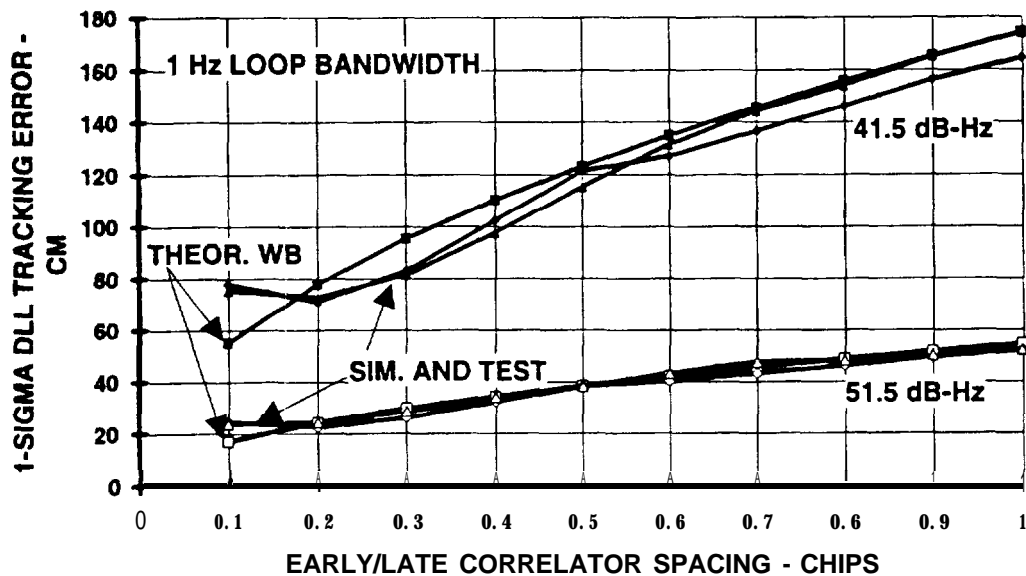


Fig. 5-Dot-Product DLL (1 Hz bandwidth) Tracking Performance Versus Spacing (noise only)

To determine the performance for other loop noise bandwidths, one simply multiplies the ordinate axis of Figure 5 by the square root of the loop bandwidth. We have baselined a bandwidth of 0.05 Hz (multiply by 0.2236) to achieve the better than 10 cm accuracy at nominal C/N_0 values, which are usually above 45 dB-Hz. This bandwidth represents a loop time constant of 5 s, which is more than wide enough to track the code-carrier divergence due to the ionosphere in the carrier-aided DLL. In fact, further smoothing would yield even better results. However, the overall tracking performance is limited by the effects of multipath, which are discussed below.

MULTIPATH EFFECTS

Although the narrow correlator spacing produces superior noise performance in a DLL, it has been noted that multipath effects in a DLL tend to dominate the error budget using the C/A-code. Comments received after the presentation of [6] emphasized this problem. However, it was suspected that the narrow spacing would also reduce the effects of multipath. This is because distortion of the cross-correlation function near its peak due to multipath is less severe than that at regions away from the peak. Thus, it was reasoned that, if one could track near the peak, the effects of multipath would be reduced. This reasoning had to be verified. The results of that verification are presented here.

In [2] it was indicated that narrow spacing did not reduce the maximum ranging error due to multipath. However, that statement was made with respect to coherent DLLs, which are more susceptible to carrier phase tracking error. This is true because the phase-lock-loop (PLL), which is required when using a coherent DLL, is tracking the composite true + multipath signal. Thus, coherent is not really coherent to the true signal, and extreme cross-correlation function distortion can occur, even with narrow spacing. The results presented in [2] were verified to be true for strong multipath returns, which will be discussed later.

It was found, however, that this statement did not apply to noncoherent DLLs. This is because those types of discriminators cancel most reliance on carrier phase, and work even when the carrier phase is not being tracked. Thus, our investigations were directed to determining the effects of multipath in noncoherent DLLs. Since we have baselined the dot-product DLL, the investigations are limited to that discriminator. However, dot-product DLL performance in a multipath environment is essentially the same as the early-minus-late power DLL for what is called Region I tracking [7]. For C/A-code applications, this is the only region of interest, since carrier aiding should never allow a transfer to Region II. Generally speaking, in Region II the multipath signal itself is being tracked, while in Region I, the multipath is simply causing a signal tracking error by distorting the discriminator [2,7].

Multipath Error Analysis

The composite true + multipath signal is given as

$$S_m(t) = AC_r(t) \cos(\omega_0 t + \phi) + \alpha AC_r(t - \delta) \cos[\omega_0(t - \delta) + \phi] \quad (8)$$

where A is the signal amplitude, $C_r(t)$ is the filtered PN code, ω_0 is the carrier frequency, ϕ is the carrier phase, α is the relative multipath signal amplitude,

and δ is the relative time delay of the multipath signal with respect to the receipt of true signal. Theoretically, α can take on values greater than unity, but practically, it will be somewhat less than unity for two reasons. The first is that the reflected multipath signal is linearly polarized, and thus attenuated by 3 dB in a right-hand-circular-polarized (RHCP) antenna. The second is that multipath is normally received through the negative gain portions of an antenna with respect to the gain through which the true signal is received. Of course, there are always non-normal situations. Note that the phase of the multipath signal differs from the true signal phase by $\omega_0\delta$.

Equation (8) essentially reflects the signal model used in [2] and [7], with the exception that, here, we are filtering the code. This is important when we narrow the correlator spacing, because the bandwidth affects the multipath distortion. If we process equation (8) in terms of I and Q samples similar to those in equations (A-1) and (A-2) of the appendix, we obtain the correlated noise-free samples

$$I_k = \sqrt{2 S/N_0 T} R_f(\tau_k) \cos\phi_k + \alpha\sqrt{2 S/N_0 T} R_f(\tau_k - \delta) \cos(\phi_m + \phi_k) \quad (9)$$

$$Q_k = \sqrt{2 S/N_0 T} R_f(\tau_k) \sin\phi_k + \alpha\sqrt{2 S/N_0 T} R_f(\tau_k - \delta) \sin(\phi_m + \phi_k) \quad (10)$$

where ϕ_m is the relative phase between the multipath component and the signal component, and $R_f(\cdot)$ is the cross-correlation function between the reference code and incoming filtered code.

Coherent DLL

If we apply the coherent discriminator of equation (3), the composite discriminator becomes

$$E[d\tau_k] = \sqrt{2 S/N_0 T} [R_f(\tau_k - d/2) - R_f(\tau_k + d/2)] \cos\phi_k + \alpha\sqrt{2 S/N_0 T} [R_f(\tau_k - \delta - d/2) - R_f(\tau_k - \delta + d/2)] \cos(\phi_m + \phi_k) \quad (11)$$

For a ϕ_m of 180 deg and an α of unity, equation (11) is identically zero for a large range of τ_k , depending upon the multipath delay and correlator spacing when the spacing is less than 1.0 chip. Thus, for the period of time these conditions occur, the DLL would not be tracking at all. This was the phenomenon that prompted the dishonorable mention for narrow spacing in [2]. However, that phenomenon would be rare and does not occur in the case of noncoherent DLLs. The analysis to follow will be only for the noncoherent case.

Noncoherent DLL

By then applying equation (2) and normalizing with $2S/N_0T$, the resulting dot-product discriminator output becomes [7]

$$\begin{aligned} E[d\tau_k] = & [R_f(\tau_k - d/2) - R_f(\tau_k + d/2)]R_f(\tau_k) \\ & + \alpha^2[R_f(\tau_k - \delta - d/2) - R_f(\tau_k - \delta + d/2)]R_f(\tau_k - \delta) \\ & + \alpha[R_f(\tau_k - d/2) - R_f(\tau_k + d/2)]R_f(\tau_k - \delta) \cos\phi_m \\ & + \alpha[R_f(\tau_k - \delta - d/2) - R_f(\tau_k - \delta + d/2)]R_f(\tau_k) \cos\phi_m \end{aligned} \quad (12)$$

Since the GPSCard™ implementation uses a discriminator that is normalized with the punctual power, the discriminator in equation (12) is normalized with the square of the multipath-distorted punctual cross-correlation function, which takes on the form [2]

$$R_{mf}^2(\tau_k) = R_r^2(\tau_k) + 2\alpha R_r(\tau_k)R_r(\tau_k - \delta) \cos\phi_m + \alpha^2 R_r^2(\tau_k - \delta), |\tau_k| \leq 1$$

$$= \alpha^2 R_r^2(\tau_k - \delta) \cos^2\phi_m, |\tau_k| > 1 \tag{13}$$

Plots of the normalized discriminator equation versus τ_k for a multipath delay of 0.5 chip and three values of ϕ_m are given in Figures 6 and 7 for a set to 0.5 and two values of d (1.0 and 0.1 chip, respectively). The filter bandwidth in the 0.1 chip case is that of the GPSCard™ (8 MHz), while the bandwidth

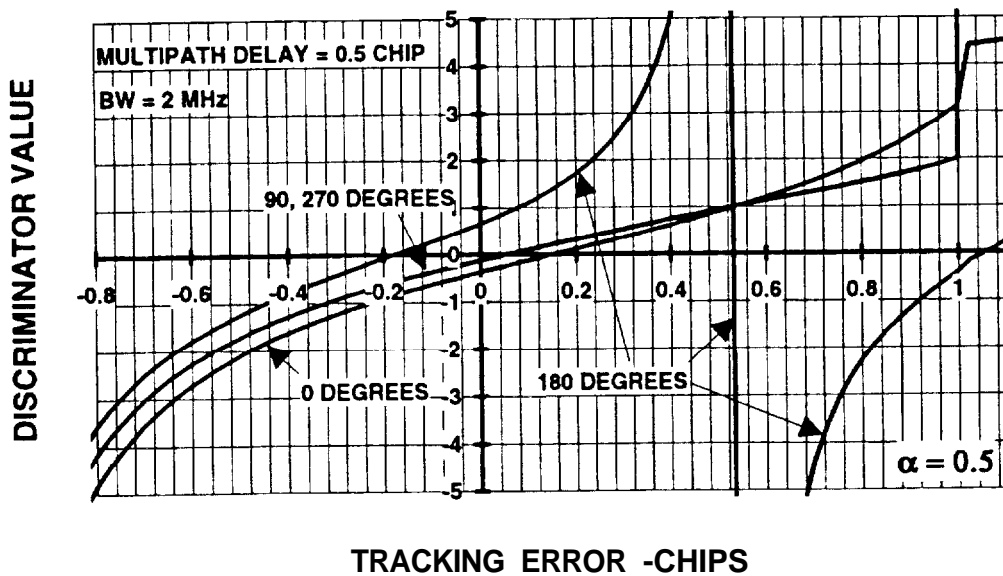


Fig. 6-Discriminator Multipath Distortion for 1.0 Chip Spacing

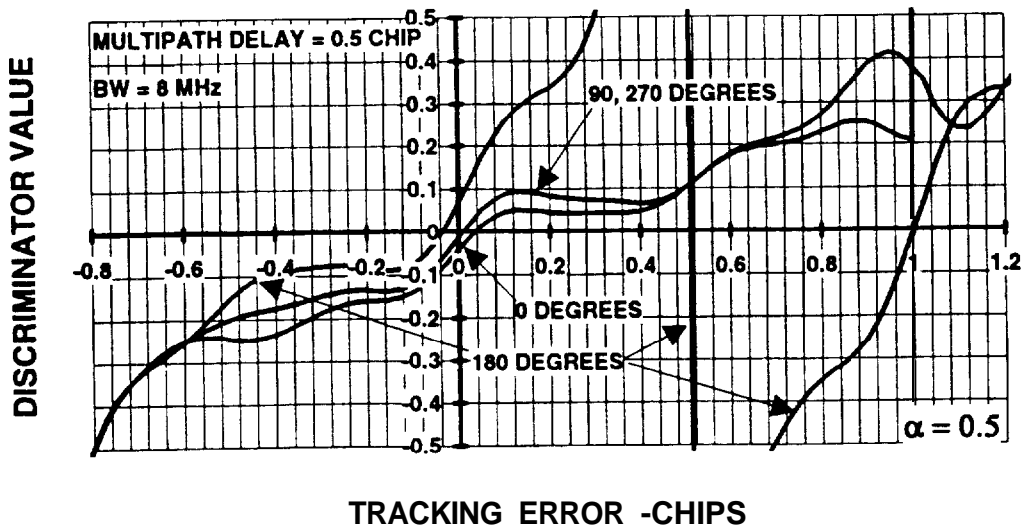


Fig. 7-Discriminator Multipath Distortion for 0.1 Chip Spacing

for the 1.0 chip case is set at a typical bandwidth for a conventional C/A-code receiver (2 MHz). Note that when the discriminator output is zero, the sign of τ_k changes as a function of the multipath phase, and varies much more for the larger correlator spacing. These figures emphasize the discriminator distortion due to multipath. Note also that for ϕ_m of 180 deg, there are other larger values of τ_k for which the discriminator is zero. This is known as Region II. However, as stated earlier, this region is of no interest. Note also that the maximum (positive) and minimum (negative) errors occur when the relative multipath phase is 0 and 180 deg, respectively. Thus, it suffices to evaluate the discriminator at those values only, producing an envelope of the multipath error versus multipath delay. Varying relative phase causes the tracking error to take on all values inside the envelope for a given multipath delay.

To evaluate the tracking error envelope versus multipath delay, equation (12) is set to zero and solved in an iterative manner for τ_k . Its value is determined for ϕ_m set to 0 and 180 deg and α set to 0.5. This is done for the two cases presented above in Figures 6 and 7, as well as for a 20 MHz bandwidth P-code using 1.0 P-code chip correlator spacing. The results are plotted in Figure 8. The evaluation for the P-code shows up as a very small region at less than 0.15 C/A chip multipath delay. The 0.1 chip error envelope is indeed much smaller than that for 1.0 chip spacing, but not as small as the P-code error envelope, for two reasons. First, the CIA-code correlates with the multipath signal with up to 10 times the delay than is the case with the P-code. Second, the 8 MHz bandwidth limits the reduction of the multipath effect.

To evaluate what would happen if the bandwidth were opened up to 20 MHz with a spacing of 0.05 chip, the same process is repeated for that case. The results are shown in Figure 9. Note that for the region of 0.15 chip multipath delay or less, the small C/A-code correlator spacing slightly outperforms the conventional P-code performance. Although the existing GPSCardTM does not have this 20 MHz capability, it is certainly a consideration for future development.

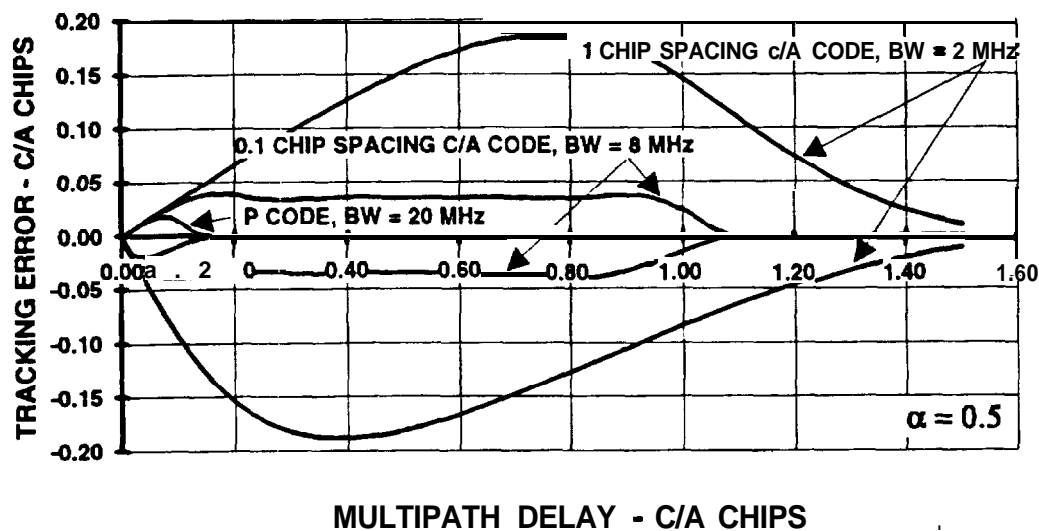


Fig. 8—Multipath Error Envelopes for 0.1 and 1.0 Chip Spacing and P-Code

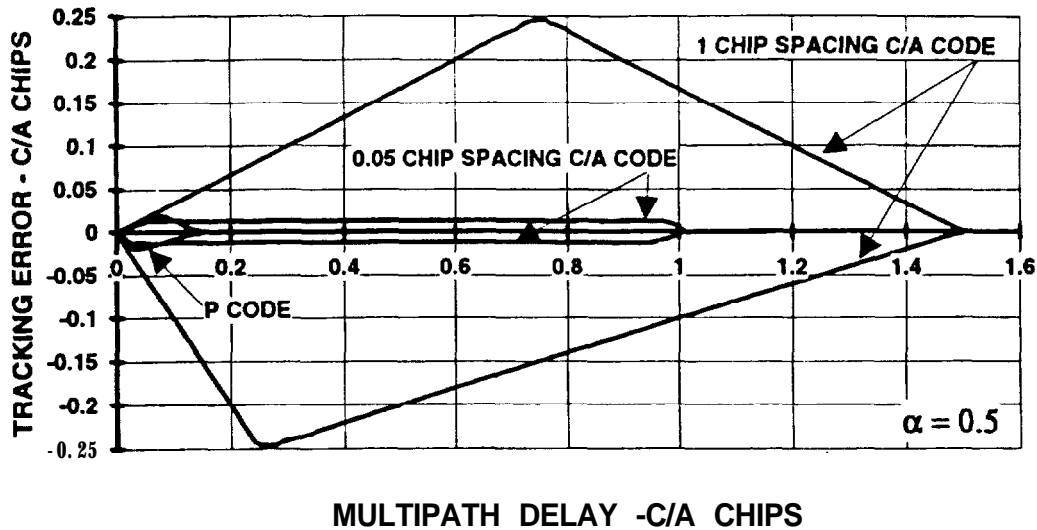


Fig. 9-Multipath Error Envelopes with 20 MHz Bandwidth

Test Results in a Multipath Environment

To verify the theory derived above on the effects of multipath, we set up an experiment on the roof of NovAtel's headquarters in Calgary, where multipath was known to exist because of many reflecting objects. In this experiment, four GPS receivers were connected to a common antenna/preamplifier. One of the purposes of the experiment was to compare the effects of multipath on C/A-code and P-code operation. Thus, two Ashtech P-12 receivers were loaned to us by The University of Calgary. The other two receivers were GPSCard™. The common antenna/preamplifier was that of one of the Ashtech receivers so as to provide data on both the L1 and L2 frequencies. Multiple satellites were tracked in each receiver. The Ashtech receivers were set up to track the P-code on both L1 and L2 and the C/A-code on L1 with an output data rate of 0.2 Hz. The NovAtel receivers were set up to track the same satellites using different correlator spacings.

First, we analyzed the collected data to find sections of the data that had obvious multipath effects, and to ensure that data were available for each of the variations described above. For a selected section of data, the code pseudorange measurements (PR) and the carrier phase measurements (ADR) were differenced to remove satellite motion and receiver and satellite clock effects. Thus, the results had a constant bias, plus the code-carrier divergence due to the ionosphere. L2 differences were compared with the L1 differences to verify that the supposed multipath effects were not ionosphere effects. Processed raw measurement data for the Ashtech L1 P-code, and the GPSCard™ C/A-code with 0.1 chip correlator spacing and with 1.0 chip spacing are shown in Figure 10. The biases in the data are arbitrary for the purpose of separating the plots. In the case of the GPSCard™, the tracking loop bandwidth was set at 0.05 Hz. The ramping of all the data over the last hour is due to the ionospheric code-carrier divergence; over this time the elevation angle varies from 40 to 16 deg. Data collection ended at that time because the Ashtech data buffer was full.

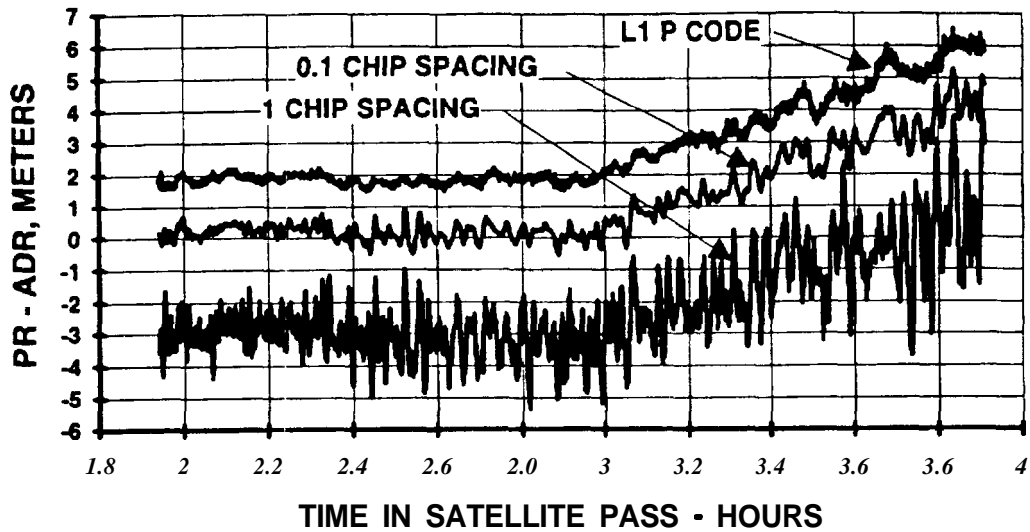


Fig. 10-Raw Measurement Data in Multipath Environment (biases are arbitrary)

The multipath effects are most noticeable in the P-code and 0.1 chip spacing data for which the noise does not dominate. For a better observation, the data presented in Figure 10 were smoothed through a first-order digital filter with a 100 s time constant. The resulting data are shown in Figure 11. Although a small portion of the multipath effects may also have been filtered, the difference in the effects due to correlator spacing is indeed noticeable. The data also show that the effects using the P-code and the C/A-code with 0.1 chip spacing are almost identical. The general difference in the effects between the P-code and C/A-code with 1.0 chip spacing agrees with data observed by other sources [8, 9].

To further identify the multipath effects, the C/A-code measurements were differenced with the P-code measurements, thus removing the effects of the

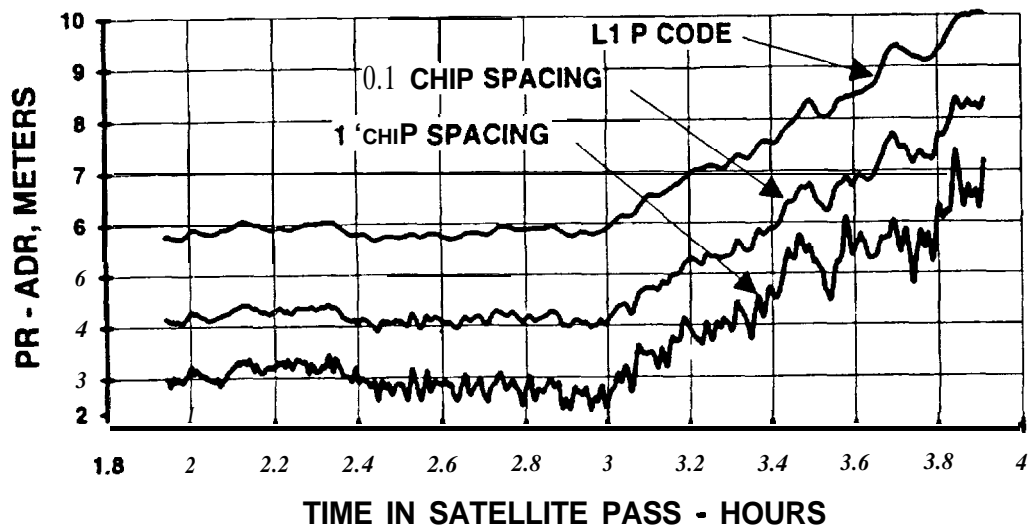


Fig. 11-Smooth Measurement Data in Multipath Environment (biases are arbitrary)

ionosphere. The results of that further differencing are shown in Figure 12, along with some statistics computed on those differences. Again, the biases are arbitrary for better viewing. The statistics were computed using only the last 36 min to provide a better gauge of the multipath effects. The range numbers are differences between the maximum and the minimum. Note that the statistics for the 1.0 chip spacing are about 3-4 times those for the 0.1 chip spacing. This is about the same as the usually observed difference between conventional C/A-code tracking and P-code tracking [8,9]

Other Testing

The GPSCard™ using the 0.1 chip spacing has also been tested in static and kinematic surveying applications by The University of Calgary. The results of that testing show remarkable agreement with the results presented here [10].

CONCLUSIONS

The theory and performance of narrow early-late correlator spacing delay lock loops (DLLs) have been presented. Remarkable performance advantages over the conventional 1.0 chip spacing DLL have been shown. The same is true in the presence of multipath. The following observations can be made:

- 1) The noise performance is proportional to the square root of the spacing, provided sufficient precorrelation bandwidth is available.
- 2) For noncoherent DLLs, the maximum multipath errors are directly proportional to the spacing, but conditioned to the availability of precorrelation bandwidth. For coherent DLLs, this observation is not necessarily true under conditions of strong multipath reception. The error envelope is also shortened by the narrower spacing, decreasing the radius to the objects that cause multipath.

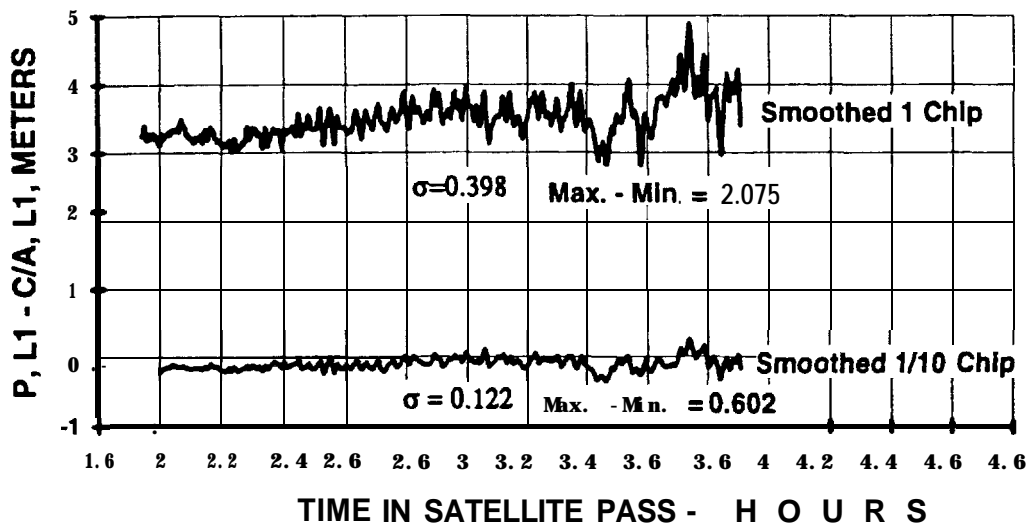


Fig. 12-Smoothed Differences Between L1 P-Code and L1 C/A-Code Measurements (biases are arbitrary)

- 3) The performance of a C/A-code receiver with a 0.1 chip correlator spacing and an 8 MHz precorrelation bandwidth is nearly as good as that of a P-code receiver.
- 4) The performance can be further enhanced by at least a factor of 3 by increasing the precorrelation bandwidth to 20 MHz and narrowing the correlator spacing to 0.05 chip.

APPENDIX DELAY LOCK LOOP NOISE PERFORMANCE DERIVATION

In this appendix we derive in four steps the equations for the noise performance of a DLL with the correlator spacing as an input variable. First, we present early, late, and punctual signal and noise models in the form of in-phase and quadrature components. Second, we derive the distortion of the signal cross-correlation function due to filtering the input signal. Then, we derive the correlation properties of the early, late, and punctual noise components. Finally, using these models and derived quantities, we derive the DLL noise performance.

Signal and Noise Models

We assume here that the receiver is tracking the carrier and removes Doppler frequency uncertainty effects. This is true for the **GPSCard™**, which phase rotates the I and Q samples before the cross-correlation process shown in Figure 1. This rotation is based on frequency and phase estimates generated in the carrier tracking loop. In a digital receiver, the I and Q components of the signal $\mathbf{S}_r(t)$, sampled at time t_k , when summed over T seconds, take on the form

$$I_k = \sqrt{2 S/N_0 T} R_r(\tau_k) \cos \phi_k + \eta_{Ik} \quad (\text{A-1})$$

$$Q_k = \sqrt{2 S/N_0 T} R_r(\tau_k) \sin \phi_k + \eta_{Qk} \quad (\text{A-2})$$

where $S/N_0 T$ is the signal-to-noise ratio in a predetection bandwidth of $1/T$ Hz (usually 50 Hz), and ϕ_k is the residual phase tracking error at time t_k . τ_k is the code tracking error at that time; $R_r(\tau_k)$ is the cross-correlation between the incoming filtered signal PRN code and the unfiltered reference code; and η_{Ik} and η_{Qk} are the in-phase and quadrature noise samples, respectively.

Equations (A-1) and (A-2) represent a normalized signal and noise model, so that the noise samples are Gaussian random variables with unity variance and zero mean. Furthermore, the I and Q noise samples (η_{Ik} and η_{Qk}) are statistically independent. However, it will be shown later that the early and late or early-minus-late and punctual samples are, in general, correlated.

The cross-correlation function describing the correlation between the reference code and the incoming signal code of the same PRN number is, in general,

$$R_r(\tau_k) = \frac{1}{\sqrt{N}} \int_0^{\infty} R(u) h(\tau_k - u) du \quad (\text{A-3})$$

where

$$\begin{aligned} R(u) &\approx 1 - |u|, \quad |u| \leq 1 \\ &\approx 0, \quad |u| > 1 \end{aligned} \quad (\text{A-4})$$

is the unfiltered PRN code autocorrelation function, and $h(\cdot)$ is the impulse response of the receiver's precorrelation filter. The normalized post-correlation noise power is

$$N = \int_{-x}^x S_c(f) |H(jf)|^2 df \quad (\text{A-5})$$

which accounts for the fact that the precorrelated noise is also filtered, where

$$S_c(f) = \frac{1}{T_c} \frac{\sin^2 \pi f T_c}{(\pi f T_c)^2} \quad (\text{A-6})$$

is the spectral density envelope of the CIA-code with $1/T_c$ equal to 1.023 MHz, and $H(jf)$ is the Fourier transform of the filter's impulse response. If $H(0)$ is 1, then $N \leq 1$. This allows the variance of the noise samples in equations A-1 and A-2 to remain at unity.

The I and Q samples of equations A-1 and A-2 represent the punctual samples (I_{Pk} and Q_{Pk}). These equations also apply to the early and late samples (I_{Ek} , Q_{Ek} , I_{Lk} , and Q_{Lk}) and early-minus-late samples ($I_{E-L,k}$ and $Q_{E-L,k}$) with the following substitutions:

$$R_r(\tau_k) = R_r(\tau_k - d/2), \quad (\text{early}) \quad (\text{A-7})$$

$$R_r(\tau_k) = R_r(\tau_k + d/2), \quad (\text{late}) \quad (\text{A-8})$$

$$R_r(\tau_k) = R_r(\tau_k - d/2) - R_r(\tau_k + d/2), \quad (\text{early-minus-late}) \quad (\text{A-9})$$

for early-late correlator spacing d in chips for early, late, and **early-minus-late**, respectively. For the I and Q noise samples of equations A-1 and A-2,

$$\eta_{Ik} = \eta_{IEk}, \quad \eta_{Qk} = \eta_{QEk}, \quad (\text{early}) \quad (\text{A-10})$$

$$\eta_{Ik} = \eta_{ILk}, \quad \eta_{Qk} = \eta_{QLk}, \quad (\text{late}) \quad (\text{A-11})$$

$$\eta_{Ik} = \eta_{IELk}, \quad \eta_{Qk} = \eta_{QELk}, \quad (\text{early-minus-late}) \quad (\text{A-12})$$

for early, late, and early-minus-late, respectively. The statistics of these noise samples take on a different meaning now, because the early and late samples are, in general, correlated.

The correlation between the early and late noise samples is independent of the fact that the noise is filtered prior to the cross-correlation process. This is because the noise is spread by the reference code (which is not filtered). In fact, the early and late or punctual and early-minus-late noise samples are based on the same incoming noise, but are spread with a different phase (or phase difference) of the code. Thus, any statistical independence in time that they might have is due only to the code. In a conventional receiver with a 1.0 chip correlator spacing, the early and late noise samples are independent. However, with the narrower spacing, they are correlated as follows:

$$\rho_{EL} = R(d) = 1 - d \quad (\text{A-13})$$

$$\rho_{E-L,P} = 0 \quad (\text{A-14})$$

The correlation between the early-minus-late and punctual noise samples is zero because the individual noise pairs (early, punctual and punctual, late)

are correlated by the same $1 - d/2$, which cancels. The variances of the early-minus-late samples are then

$$\mathbf{E}[\eta_{iELk}^2] = \mathbf{E}[\eta_{qELk}^2] = 2 - 2(1 - d) = 2d \quad (\text{A-15})$$

where $\mathbf{E}[\cdot]$ is the expected value operator.

DLL Discriminator Statistics

Using the models given in equations (1) and (2) of this paper for the **noncoherent** DLL discriminators, we have their expected values

$$\begin{aligned} \mathbf{E}[d\tau_k] &= \mathbf{I}_{Ek}^2 + \overline{\mathbf{Q}}_{EK}^2 - \mathbf{I}_{Lk}^2 - \overline{\mathbf{Q}}_{Lk}^2 \\ &= 2 S/N_o T [\mathbf{R}_r^2(\tau_k - d/2) - \mathbf{R}_r^2(\tau_k + d/2)] \end{aligned} \quad (\text{A-16})$$

$$\begin{aligned} \mathbf{E}[d\tau_k] &= \mathbf{I}_{E-L,k} \mathbf{I}_{Pk} + \overline{\mathbf{Q}}_{E-L,k} \overline{\mathbf{Q}}_{Pk} \\ &= 2 S/N_o T [\mathbf{R}_r(\tau_k - d/2) - \mathbf{R}_r(\tau_k + d/2)] \mathbf{R}_r(\tau_k) \end{aligned} \quad (\text{A-17})$$

for the early-minus-late power and dot-product modes, respectively. For the coherent case of equation (3), if phase lock is maintained with no data bit demodulation errors, we have its expected value

$$\begin{aligned} \mathbf{E}[d\tau_k] &\approx \mathbf{I}_{E-L,k} \\ &= \sqrt{2 S/N_o T} [\mathbf{R}_r(\tau_k - d/2) - \mathbf{R}_r(\tau_k + d/2)] \end{aligned} \quad (\text{A-18})$$

In the infinite precorrelation bandwidth case, equations (A-16), (A-17), and (A-18) reduce further for $|\tau_k| \leq d/2$ to

$$\mathbf{E}[d\tau_k] = 4 S/N_o T (2 - d)\tau_k, \text{ (early-minus-late power)} \quad (\text{A-19})$$

$$\mathbf{E}[d\tau_k] = 4 S/N_o T \tau_k (1 - |\tau_k|), \text{ (dot-product)} \quad (\text{A-20})$$

$$\mathbf{E}[d\tau_k] \approx 2\sqrt{2 S/N_o T} \tau_k, \text{ (coherent)} \quad (\text{A-21})$$

The evaluation of the variances of the noncoherent discriminators requires a fair amount of algebra, especially for the early-minus-late power discriminator. The key relationship in those evaluations is the fact that, for correlated Gaussian random variables 1111,

$$\mathbf{E}[\mathbf{x}_1 \mathbf{x}_2 \mathbf{x}_3 \mathbf{x}_4] = \mathbf{E}[\mathbf{x}_1 \mathbf{x}_2] \mathbf{E}[\mathbf{x}_3 \mathbf{x}_4] + \mathbf{E}[\mathbf{x}_1 \mathbf{x}_3] \mathbf{E}[\mathbf{x}_2 \mathbf{x}_4] + \mathbf{E}[\mathbf{x}_1 \mathbf{x}_4] \mathbf{E}[\mathbf{x}_2 \mathbf{x}_3] \quad (\text{A-22})$$

Also, to evaluate those variances with filtered cross-correlation functions, as given in equation (A-3), would be extremely messy. That is left for computer simulation, results of which are presented in the paper. The evaluation using infinite precorrelation bandwidths, although tedious, yields the following:

$$\sigma_{d\tau_k}^2|_{\tau_k=0} = 4d(2 - d)[(2 - d)S/N_o T + 2], \text{ (early-minus-late power)} \quad (\text{A-23})$$

$$\sigma_{d\tau_k}^2|_{\tau_k=0} = 4d(S/N_o T + 1), \text{ (dot-product)} \quad (\text{A-24})$$

$$\sigma_{d\tau_k}^2|_{\tau_k=0} = 2d, \text{ (coherent)} \quad (\text{A-25})$$

These variances are only those of the open-loop discriminators, and do not reflect the tracking errors of the DLLs themselves. To evaluate those, we must close the loop.

Closed-Loop Statistics

For a carrier-aided DLL, it suffices to use a first-order loop. For a first-order loop, the closed-loop noise time-update error (T,J equation is of the form

$$\tau_{k+1} = (1 - 4B_L T)\tau_k + K_L d\tau_k \quad (\text{A-26})$$

where B_L is the loop noise bandwidth, and the loop update rate equals the I and Q sample rate. The loop gain K_L is normalized as

$$K_L = \frac{4B_L T \tau_k}{E[d\tau_k]} \Big|_{\tau_k=0} \quad (\text{A-27})$$

so that the correct bandwidth is achieved. For example, the loop gain for the dot-product discriminator is

$$K_L = \frac{4B_L T}{4 S/N_o T} = \frac{B_L}{S/N_o} \quad (\text{A-28})$$

The variance time-update equation for zero mean tracking error is then

$$\sigma_{\tau,k+1}^2 = (1 - 4B_L T)^2 \sigma_{\tau,k}^2 + K_L^2 \sigma_{d\tau,k}^2 \Big|_{\tau_k=0} \quad (\text{A-29})$$

However, in steady state,

$$\sigma_{\tau}^2 = \sigma_{\tau,k+1}^2 = \sigma_{\tau,k}^2 \quad (\text{A-30})$$

so that

$$\sigma_{\tau}^2 = \frac{K_L^2}{8B_L T(1 - 2B_L T)} \sigma_{d\tau}^2 \approx \frac{K_L^2}{8B_L T} \sigma_{d\tau}^2 \quad (\text{A-31})$$

for $B_L T \ll 1$. Thus, for the three discriminators, the closed-loop noise variances are

$$\sigma_{\tau}^2 = \frac{B_L d}{2 \text{SIN}} \left[1 + \frac{2}{(2-d) S/N_o T} \right], \text{ (early-minus-late power)} \quad (\text{A-32})$$

$$\sigma_{\tau}^2 = \frac{B_L d}{2 S/N_o} \left[I + \frac{1}{S/N_o T} \right], \text{ (dot-product)} \quad (\text{A-33})$$

$$\sigma_{\tau}^2 \approx \frac{B_L d}{2 \text{SIN}}, \text{ (coherent)} \quad (\text{A-34})$$

The second term in the brackets for the noncoherent discriminators represents squaring loss, which is always less for the dot-product discriminator. However, that loss is significant only at very low signal-to-noise ratios that are more typical in a jamming environment. In that type of environment, the equation for the coherent loop would no longer be valid, because the data bit error rate would be too high.

Note that the performance of the three types of discriminators is the same at signal-to-noise ratios that are typical for commercial GPS applications. In each case, for the infinite bandwidth assumption, the standard deviation of the tracking error varies with the square root of the correlator spacing, the phenomenon that we set out to prove in this appendix. However, it is shown in the paper that a diminishing return is realized with very narrow spacing because of precorrelation bandwidth constraints.

ACKNOWLEDGMENT

The authors express their appreciation to Dr. Gérard Lachapelle and The University of Calgary for loaning us the Ashtech P12 receiver for testing.

REFERENCES

1. Spilker, J. J., Jr., **GPS Signal Structure and Performance Characteristics**, Global Positioning System, Volume I, The Institute of Navigation, 1980, pp. 29-54.
2. Hager-man, L. L., **Effects of Multipath on Coherent and Noncoherent PRN Ranging Receiver**, Aerospace Corporation Report No. TOR-0073(3020-03)-3, 15 May 1973.
3. Private communication with L. L. Hager-man and with M. S Braasch of The Ohio University.
4. Frank, G. B. and Yakos, M. D., **Collins Next Generation Digital GPS Receiver**, Record of the IEEE 1990 Position Location and Navigation Symposium, PLANS 90, Las Vegas, NV, 21-23 March 1990, pp. 286-92.
5. Moyle, C., Thomas, J., and Leasure, S., **Architecture and Field Test Results of a Digital GPS Receiver**, Proceedings of the Satellite Division First Technical Meeting, The Institute of Navigation, Colorado Springs, CO, 23-25 September 1987, pp. 119-29.
6. Fenton, P., Falkenberg, B., Ford, T., Ng, K., and Van Dierendonck, A. J., **NovAtel's GPS Receiver-The High Performance OEM Sensor of the Future**, Proceedings of ION GPS-91, Fourth International Technical Meeting of the Satellite Division of The Institute of Navigation, Albuquerque, NM, 11-13 September 1991, pp. 49-58.
7. Natali, F.D., **Comparison of the Noncoherent Delay-Lock Loop and the Data Estimating Delay-Lack Loop in the Presence of Specular Multipath**, Stanford Telecommunications, Inc., Report No. STI-TR-33048,5 April 1983.
8. Hatch, R., Magnavox, private communication.
9. Lachapelle, G., Falkenberg, W., Neufeldt, D., and Kielland, P., **Marine DGPS Using Code and Carrier in a Multipath Environment**, Proceedings of ION GPS-89, Second International Technical Meeting of the Satellite Division of The Institute of Navigation, Colorado Springs, CO, 27-29 September 1989, pp. 343-47.
10. Cannon, M. E. and Lachapelle, G., **Analysis of a High-Performance C/A-Code GPS Receiver in Land Kinematic Mode**, this issue of NAVIGATION.
11. Brown, R. G. and Hwang, I? Y. C., **Introduction to Random Signals and Applied Kalman Filtering, Second Edition**, John Wiley and Sons, Inc., 1991.